crystals

MDPI

Article

The Synthesis and Crystallographic Characterization of Emissive Pt(II) and Au(I) Compounds Exploiting the 2-Ethynylpyrimidine Ligand

Sarah L. McDarmont [1], Mary Jo McCormick [2], Paul S. Wagenknecht [2], Lily E. Duplooy [3], Jared A. Pienkos [1,*] and Colin D. McMillen [4,*]

[1] Department of Chemistry and Physics, The University of Tennessee at Chattanooga, Chattanooga, TN 37403, USA
[2] Department of Chemistry, Furman University, Greenville, SC 29613, USA
[3] Girls Preparatory High School, Chattanooga, TN 37405, USA
[4] Department of Chemistry, Clemson University, Clemson, SC 29634, USA
* Correspondence: jared-pienkos@utc.edu (J.A.P.); cmcmill@clemson.edu (C.D.M.)

Abstract: The luminescent properties of Au(I) and Pt(II) compounds are commonly tuned by exploiting the alkynyl ligand with varying electron density. Herein, we describe the synthesis of three new emissive transition metal compounds, ^{t}bpyPt(C_2pym)$_2$, Ph_3PAuC_2pym, and Cy_3PAuC_2pym (where HC_2pym = 2-ethynylpyrimidine), verified by ^{1}H-NMR, EA, and a single-crystal X-ray diffraction analysis. The ^{t}bpyPt(C_2pym)$_2$ complex crystallized as an Et_2O solvate in the orthorhombic space group *Pbca* with Z = 24 with three unique Pt(II) species within the unit cell. The Cy_3PAuC_2pym species crystallizes in a monoclinic space group with one unique complex in the asymmetric unit. Changing the identity of the phosphine from Cy_3P to Ph_3P influences interactions within the unit cell. Ph_3PAuC_2pym, which also crystalizes in a monoclinic space group, has an aurophilic bonding interaction Au–Au distance of 3.0722(2) Å, which is not present in crystalline Cy_3PAuC_2pym. Regarding optical properties, the use of an electron-deficient heterocycle provides an alternate approach to blue-shifting the emission of Pt(II) transition metals' compounds, where the aryl moiety is made more electron-deficient by exploiting nitrogen within this moiety instead of the typical strategy of decorating the aryl ring with electron withdrawing substituents (e.g., fluorines). This is indicated by the blue-shift in emission that occurs in ^{t}bpyPt(C_2pym)$_2$ (λ_{max}, emission = 512 nm) compared to the previously reported ^{t}bpyPt($C_2$2-py)$_2$ (where $HC_2$2-py = 2-ethynylpyridine) complex (λ_{max}, emission = 520 nm).

Keywords: alkyne ligands; luminescence; gold (I); platinum (II); aurophilic bonding; crystal structure

check for updates

Citation: McDarmont, S.L.; McCormick, M.J.; Wagenknecht, P.S.; Duplooy, L.E.; Pienkos, J.A.; McMillen, C.D. The Synthesis and Crystallographic Characterization of Emissive Pt(II) and Au(I) Compounds Exploiting the 2-Ethynylpyrimidine Ligand. *Crystals* **2024**, *14*, 587. https://doi.org/10.3390/cryst14070587

Academic Editor: Kil Sik Min

Received: 31 May 2024
Revised: 18 June 2024
Accepted: 21 June 2024
Published: 26 June 2024

Copyright: © 2024 by the authors. Licensee MDPI, Basel, Switzerland. This article is an open access article distributed under the terms and conditions of the Creative Commons Attribution (CC BY) license (https://creativecommons.org/licenses/by/4.0/).

1. Introduction

A systematic way to tune the emission and absorption of transition metal compounds is to modify the electronics of a pendant alkynyl ligand [1–3]. This method has been previously exploited with various Pt(II) [4,5] and Au(I) [6] compounds to generate luminescent materials, which have applications in numerous devices including OLEDs [7]. Despite progress in developing OLEDs using organometallic phosphors, the development of materials with deep blue emission still receives significant attention [8–11], and thus general strategies to blue-shift emission are important. Regarding Pt(II) species, the emission of these compounds can be blue-shifted by decreasing the electron density of the alkynyl ligand. For instance, the -$C_2C_6F_6$ ligand (where $HC_2C_6F_6$ = 1-ethynyl-2,3,4,5,6-pentafluorobenzene) is commonly used as an electron-deficient ligand to tune the emission of Pt(II) species [4,5,12] as it raises the energy of the metal-to-ligand charge-transfer (MLCT) and the ligand-to-ligand charge-transfer (LL'CT) excited states (ESs) [1,4,5,12–16]. For example, in the series of compounds ^{t}bpyPt(C_2R)$_2$ (Figure 1), the ^{t}bpyPt($C_2C_6F_5$)$_2$ complex

has the most blue-shifted emission (λ_{max} = 501 nm in CH_2Cl_2) [4,17]. The electron-deficient -$C_2C_6F_6$ ligand has also been exploited to tune Au(I) phosphors [6].

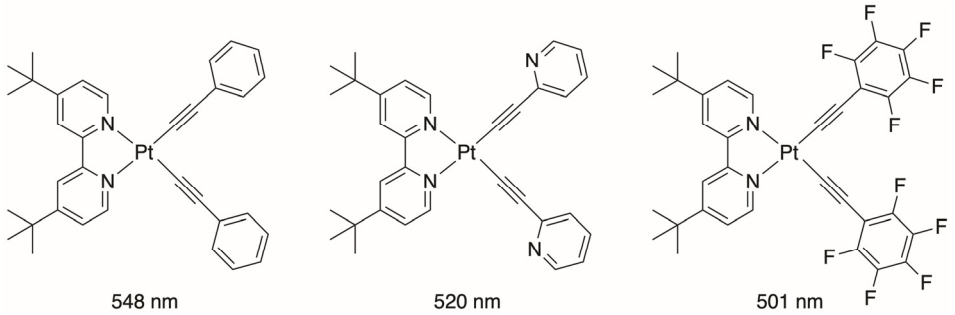

Figure 1. Pt(II) compounds of the form ^{t}bpyPt(C_2R)$_2$ (R = phenyl (**left**), pyridyl (**center**), and perfluorophenyl (**right**)) and their corresponding emission λ_{max} in CH_2Cl_2.

An alternative approach to the fluorine-substituted -$C_2C_6F_6$ ligand is the introduction of electron-deficient heteroatoms to decrease the electron density of the aryl ring appended to the alkyne. For instance, pyridine is more electron-deficient than benzene due to the presence of the nitrogen atom, and pyrazine rings containing two nitrogen atoms are even more electron-deficient. This is reflected in the basicity of the pyridine [18] and pyrazine [19,20] ring systems. In emissive transition metal compounds, the presence of the pyridyl ring in ^{t}bpyPt(C2-2py)$_2$ (where HC_2-2py = 2-ethynylpyridine) blue-shifts emission relative to the ^{t}bpyPt(C_2Ph)$_2$ derivative (Figure 1), indicating the lowering of the MLCT and LL'CT ES. Similar to the aforementioned Pt(II) alkynyl compounds, the emission of Au(I) species of the form Cy_3PAuC_2R can be blue-shifted when the alkynyl group is made more electron-deficient [21]. Herein, we describe the synthesis and characterization of three new alkynyl compounds, which exploit 2-ethynylpyrimidine (HC_2pym) to provide insight into how this electron-deficient heterocycle can impact the properties of these transition metal compounds.

2. Materials and Methods

2.1. General Methods

UV-Vis: Absorption spectra were collected using a Cary-50 UV-Vis spectrophotometer (Agilent Technologies, Santa Clara, CA, USA).

Emission spectra: Emission spectra were collected using a Horiba (Kyoto, Japan) Scientific Fluorolog-3 spectrofluorometer. All emission spectra were recorded when compound concentration was at approximately 10^{-5} M with the following excitation wavelengths: 380 nm for ^{t}bpyPt(C_2pym) and 285 nm for Ph_3PAuC_2pym and Cy_3PAuC_2pym.

Excitation spectra: Excitation spectra were collected using a Horiba (Kyoto, Japan) Scientific Fluorolog-3 spectrofluorometer using an emission assay of 525 nm for ^{t}bpyPt(C_2pym)$_2$ and 450 nm for Ph_3PAuC_2pym and Cy_3PAuC_2pym.

NMR spectra: ^{1}H NMR spectra were recorded on a JEOL (Peabody, MA, USA) ECX 400 MHz spectrometer. ^{1}H NMR resonances were referenced against tetramethylsilane using residual proton signals.

Elemental analysis: Atlantic Microlabs (Norcross, GA, USA) performed all elemental analysis measurements using a Carlo Erba (Milan, Italy) 1108 analyzer.

All reactions were performed under N_2. The compounds ^{t}bpyPtCl_2 [22], Ph_3PAuCl [23], and Cy_3PAuCl [24] were prepared according to previously reported procedures. CH_2Cl_2 and MeOH were dried with Al_2O_3 (passed through a column), (iPr)$_2$NH was distilled over KOH, and all other reagents were used as received.

^{t}bpyPt(C_2pym)$_2$: ^{t}bpyPtCl_2 (299.9 mg, 0.5612 mmol), HC_2pym (133.4 mg, 1.281 mmol), CuI (16.5 mg, 0.0866 mmol), CH_2Cl_2 (40 mL), and (iPr)$_2$NH (10 mL) were combined and the yellow mixture was stirred at rt. After 18 h, the yellow solution was dried in vacuo to give a brown solid, which was then redissolved in CH_2Cl_2 (100 mL) and washed with sat. aq. Na_2CO_3 (5 × 100 mL), H_2O (100 mL), and sat. aq. NaCl (100 mL). The organic

layer was dried over $MgSO_4$ and the solvent was removed in vacuo. The resulting solid was purified using flash chromatography (neutral Al_2O_3, ~4 cm in a 60 mL fritted glass funnel). A yellow-brown band was eluted with 5% MeOH in CH_2Cl_2, and the fraction containing this colored band was dried in vacuo, treated with Et_2O (20 mL), and sonicated, and the resulting solid was collected by filtration and washed with Et_2O (3 × 10 mL) to give ^{t}bpyPt(C_2pym)$_2$ as a yellow-brown solid (266.8 mg, 0.3984 mmol, 71%). ^{1}H-NMR ($CDCl_3$): δ 9.15 (d, *J* = 5.91 Hz, 2H), 8.65 (d, *J* = 4.91 Hz, 4 H), 8.50 (s, 2H), 7.38 (dd, *J* = 2.09, 6.04 Hz, 2 H), 7.05 (t, *J* = 4.97 Hz, 2H). UV-Vis (CH_2Cl_2): λ_{max} = 377 nm, ε = 9700. Elemental analysis (found, calculated) for $C_{30}H_{30}N_6Pt\bullet 1/2\ H_2O$, C (52.99, 53.09), H (4.89, 4.60), N (12.00, 12.38). Single crystals were grown by layering a CH_2Cl_2 solution of ^{t}bpyPt(C_2pym)$_2$ with acetone followed by Et_2O. Crystals formed within one day.

Ph_3PAuC_2pym: KOH (150.8 mg, 2.688 mmol), HC_2pym (92.7 mg, 0.890 mmol), and MeOH (13 mL) were combined. To this, a solution of PPh_3AuCl (400.1 mg, 0.8088 mmol) in 1:1 MeOH/acetone (40 mL) was added, forming a light-brown solution. After 24 h, the solvent was removed in vacuo and the resulting light-brown oil was suspended in CH_2Cl_2 (15 mL), sonicated, and filtered through celite. The celite was washed with CH_2Cl_2 (5 × 10 mL) and the collected filtrate was dried in vacuo, redissolved in minimal CH_2Cl_2 (~1 mL), and added to hexanes (20 mL). The resulting precipitate was collected by filtration and washed with hexanes (3 × 10 mL), giving Ph_3PAuC_2pym as a white solid (302.3 mg, 0.5376 mmol, 66%). ^{1}H-NMR (d_6-acetone): δ 8.64 (d, *J* = 4.96 Hz, 2H), 7.67–7.58 (m, 15 H), 7.25 (t, *J* = 4.87 Hz, 1H). UV-Vis (CH_2Cl_2): λ_{max} = 275 nm, ε = 33,000. Elemental analysis (found, calculated) for $C_{24}H_{18}AuN_2P$, C (51.19, 51.26), H (3.28, 3.23), N (4.84, 4.98). Single crystals were grown by layering a CH_2Cl_2 solution of Ph_3PAuC_2pym with toluene followed by hexanes. Crystals formed after three days.

Cy_3PAuC_2pym: KOH (90.2 mg, 1.61 mmol), HC_2pym (54.3 mg, 0.522 mmol), and MeOH (7.5 mL) were combined. To this, a solution of Cy_3PAuCl (241.8 mg, 0.4715 mmol) in 1:1 MeOH/acetone (25 mL) was added, forming a light-brown mixture. After 24 h, the solvent was removed in vacuo. The resulting light-brown oil was suspended in CH_2Cl_2 (15 mL), sonicated, and filtered through celite. The celite was washed with CH_2Cl_2 (5 × 10 mL) and the collected filtrate was dried in vacuo. The resulting white solid was treated with hexanes (20 mL) and filtered, and the collected solid was washed with hexanes (4 × 10 mL), giving Cy_3PAuC_2pym as a white solid (215.1 mg, 0.3705 mmol, 79%). ^{1}H-NMR ($CDCl_3$): δ 8.60 (d, *J* = 5.01, 2H), 7.06 (t, *J* = 4.98, 1H), 2.07–1.15 (m, 33 H). UV-Vis (CH_2Cl_2): λ_{max} =275 nm, ε = 29,000. Elemental analysis (found, calculated) for $C_{24}H_{36}AuN_2P$, C (49.43, 49.66), H (6.37, 6.25), N (4.85, 4.83). Single crystals were grown by layering a CH_2Cl_2 solution of Cy_3PAuC_2pym with toluene followed by hexanes. Crystals formed after three days.

2.2. Single-Crystal X-ray Diffraction

Single-crystal X-ray diffraction data were collected at 100 K using a Bruker (Madison, WI, USA) D8 Venture diffractometer. The data were collected using phi and omega scans (0.50° frame width) with a Mo Kα (λ = 0.71073 Å) microfocus source and Photon 2 detector. Data were integrated (SAINT) and corrected for absorption using the multi-scan technique (SADABS), both within the Apex3 suite [25]. The structures were solved by intrinsic phasing (SHELXT) and subsequently refined by full matrix least squares on F^2 (SHELXL) [26,27]. All non-hydrogen atoms were refined anisotropically. Hydrogen atoms attached to carbon atoms were refined in calculated positions using the appropriate riding models.

The ^{t}bpyPt(C_2pym)$_2$ complex was found to crystallize as the diethyl ether solvate, with 0.25 molecules of Et_2O per formula unit. Due to their partial occupancy in the structural voids, the disordered Et_2O molecules were refined using several restraints to maintain chemically reasonable interatomic distances and anisotropic displacement parameters. One of the unique solvent molecules is present in half-occupancy due to symmetry constraints and the second unique solvent molecule is present in partial (0.25) occupancy in the voids. The latter occupancy was first tested by free variable refinement and found to be very

close to 0.25, so it was fixed at this value for the final refinement. Elsewhere in this structure, disorder was observed in the orientation of two of the pyrimidine rings of the Pt1 complex and in one of the t-butyl groups of the Pt3 complex. Restraints were again employed in these instances to maintain similarity between the respective disordered contributions, where the site occupancies of the disordered parts were freely refined with a unity sum. The Ph_3PAuC_2pym complex crystallized as a dinuclear complex via aurophilic bonding and was refined in a fully ordered model without restraints. The Cy_3PAuC_2pym complex crystallized as a mononuclear complex and was likewise fully ordered and required no restraints. Crystallographic data are summarized in Table 1. CCDC 2359466–2359468 contain the complete supplementary crystallographic data for this paper and can be obtained from the Cambridge Crystallographic Data Centre.

Table 1. Crystallographic data.

	^{t}bpyPt(C_2pym)$_2$ · 0.25(Et_2O)	**Ph_3PAuC_2pym**	**Cy_3PAuC_2pym**
Formula	$C_{31}H_{32.5}N_6O_{0.25}Pt$	$C_{48}H_{36}Au_2N_4P_2$	$C_{24}H_{36}AuN_2P$
F. W. (g/mol)	688.22	1124.68	580.48
Temperature (K)	100	100	100
Crystal system	orthorhombic	monoclinic	monoclinic
Space group	*Pbca*	$P2_1/c$	$P2_1/c$
a (Å)	29.784 (3)	13.4341 (9)	9.4051 (4)
b (Å)	20.2605 (15)	13.1567 (7)	10.9640 (5)
c (Å)	30.014 (3)	23.1407 (15)	22.0930 (11)
α (°)	90	90	90
β (°)	90	97.518 (2)	91.3946 (17)
γ (°)	90	90	90
Volume (Å^3)	18,112 (3)	4045.9 (4)	2277.50 (18)
Z	24	4	4
D(calcd) (g/cm^3)	1.514	1.842	1.693
μ, mm^{-1}	4.678	7.346	6.542
F(000)	8172	2160	1152
Crystal size (mm)	0.03 × 0.04 × 0.29	0.04 × 0.14 × 0.33	0.16 × 0.16 × 0.28
θ range, °	2.23 to 25.25	2.27 to 27.50	2.62 to 28.50
Reflns. collected	195,665	79,113	55,194
Indep. reflns.	16,382	9303	5746
R (int)	0.0875	0.0494	0.0296
No. of parameters	1240	505	254
No. of restraints	691	0	0
R1, wR2 (I > 2σ(I))	0.0753, 0.1526	0.0216, 0.0525	0.0119, 0.0278
R1, wR2 (all data)	0.0885, 0.1585	0.0243, 0.0548	0.0129, 0.0283
S	1.180	1.078	1.110
Largest diff. peak/hole (eÅ^{-3})	2.465, −3.441	1.297, −1.715	0.462, −0.537
CCDC deposition no.	2359466	2359467	2359468

3. Results and Discussion

3.1. Synthesis of Alkynyl Compounds

The compounds ^{t}bpyPt(C_2pym)$_2$, Ph_3PAuC_2pym, and Cy_3PAuC_2pym were synthesized from the chloride complexes ^{t}bpyPtCl_2, Ph_3PAuCl, and Cy_3PAuCl, respectively (Scheme 1). For ^{t}bpyPt(C_2pym)$_2$, the strategy reported by Lu et al. was utilized to deprotonate HC_2pym in the presence of CuI/*i*Pr_2NH to form the desired alkynyl compound. It was found that upon purifying this species using flash chromatography often [*i*Pr_2NH_2]Cl would coelute with our desired product and remain with our product following Et_2O precipitation. Therefore, a basic extraction (aqueous Na_2CO_3) was performed to remove this amine salt prior to column chromatography. Regarding the Ph_3PAuC_2pym and Cy_3PAuC_2pym alkynyl compounds, KOH was used to deprotonate HC_2pym in an acetone/MeOH solution to form the desired Au(I) compounds. The excess KOH and the KCl by-products from these reactions were removed by dissolving the mixture in CH_2Cl_2

and filtering through a celite plug prior to precipitating (for Ph_3PAuC_2pym) or treating with hexanes (for Cy_3PAuC_2pym) to afford the desired solid.

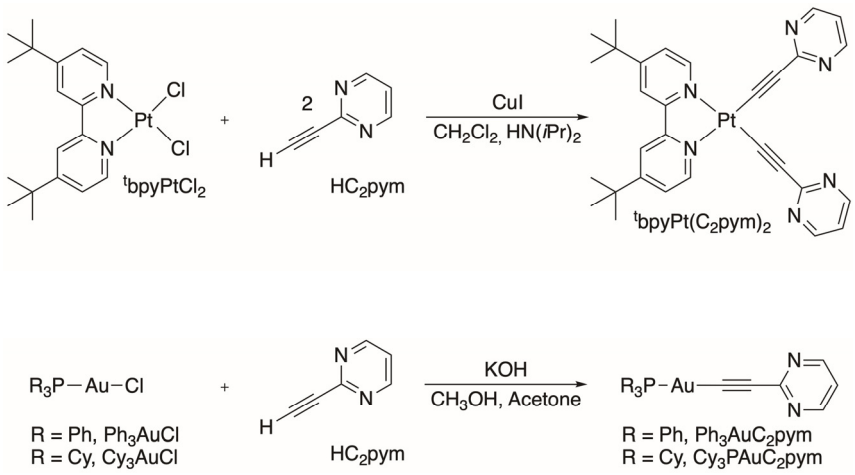

Scheme 1. Synthesis of ^{t}bpyPt(C_2pym)$_2$, Ph_3PAuC_2pym, and Cy_3PAuC_2pym.

3.2. Crystallographic Characterization

The ^{t}bpyPt(C_2pym)$_2$ complex crystallized as an Et_2O solvate in the orthorhombic space group *Pbca* with Z = 24. The asymmetric unit consists of three crystallographically unique complexes (Figure 2: Pt1, Pt2, Pt3), differing slightly in the relative rotational orientations of the pyrimidine rings and their attachment angle at the alkyne. The Pt atoms are all four-coordinate square planar with C–Pt–C angles of 91.7(5)° for Pt1, 91.0(6)° for Pt2, and 89.4(6)° for Pt3, with Pt–C ranging from 1.928(11) Å to 1.956(13) Å and Pt–N ranging from 2.038(10) Å to 2.074(10) Å. Though there are no metal complexes of *LM*(C_2pym)$_2$ coordination reported in the CSD for direct comparison, these are comparable values to those in similar *L*Pt($C_2$2-py)$_2$ (*L* = benzo(h)quinoline [28], 4,4′-di-t-butyl-2,2′-bipyridine [29], and 1-benzyl-2-(2-pyridyl)benzimidazole [30]) complexes. Also similar to the ethynylpyridine complexes, the ethynylpyrimidine complex ^{t}bpyPt(C_2pym)$_2$ here exhibits Pt–C≡C and C≡C–C bonds that can deviate from linearity to accommodate packing with neighboring molecules.

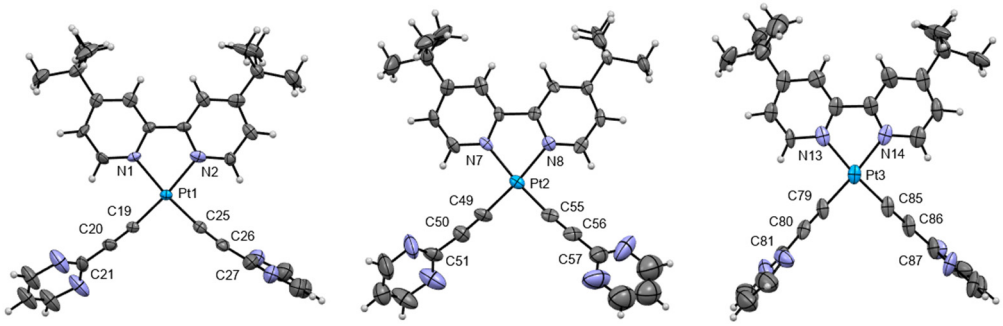

Figure 2. Three crystallographically unique complexes of ^{t}bpyPt(C_2pym)$_2$ in the structure of ^{t}bpyPt(C_2pym)$_2$ · 0.25(Et_2O), with displacement ellipsoids shown at 50% probability levels.

The complexes form stacks along the *b*-axis, with the *b*-axis length of 20.2605(15) Å comprising six complexes and the unit cell in total containing four such stacks (Figure 3). Though the mean planes of the PtN_2C_2 cores of the complexes are not formally parallel in the stacks, this spacing suggests an average distance of 3.38 Å between complexes. The orientation of the complexes alternates within these stacks via rotation in the *ac* plane, allowing the *t*-butyl groups and the ethynylpyrimidine arms to be adequately accommodated. This is a similar motif to what was observed in the ethynylpyridine complex [29], ^{t}bpyPt($C_2$2-py)$_2$ (CSD refcode RUGWIC) with a *b*-axis stacking of six complexes over

20.4987(17) Å. In that structure, all six of the complexes were crystallographically unique. The rotation of the stacked complexes in ^{t}bpyPt(C_2pym)$_2$ · 0.25(Et_2O) results in Pt···Pt distances ranging from 4.1659(7) Å to 4.3850(7) Å. The disordered Et_2O solvent molecules occupy voids between the stacks.

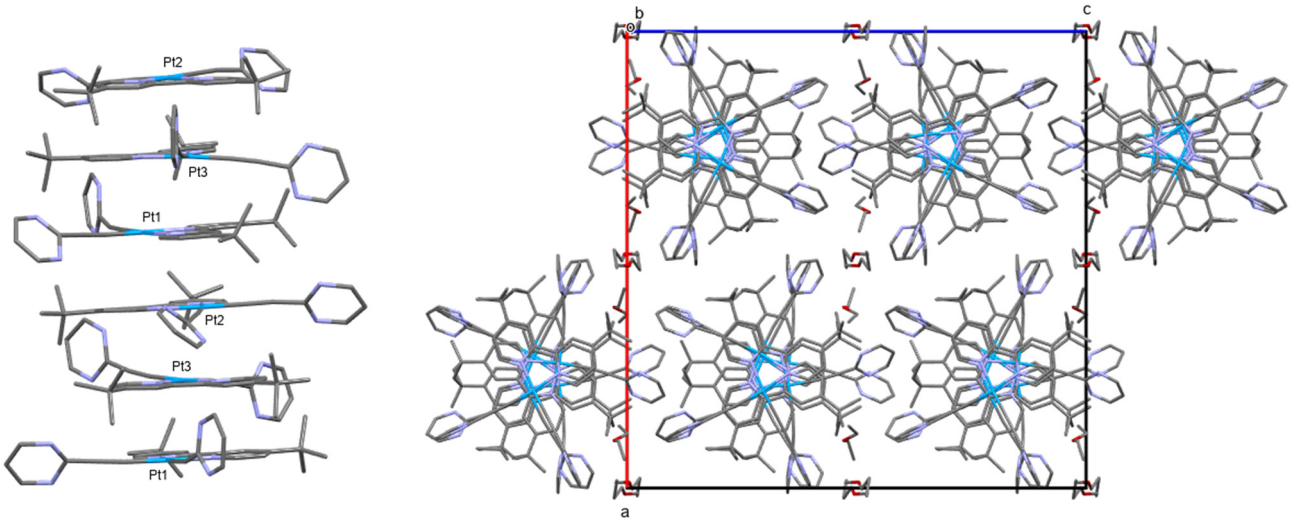

(**a**) (**b**)

Figure 3. Stacks of complexes in ^{t}bpyPt(C_2pym)$_2$ · 0.25(Et_2O): (**a**) Six complexes stack in rotated fashion, viewed as normal to *b*-axis. (**b**) Packing diagram viewed along *b*-axis. For clarity, hydrogen atoms are omitted and only major-occupied disordered contributions are shown. Carbon atoms are gray, nitrogen atoms are purple, platinum atoms are blue, and oxygen atoms (of the Et_2O molecules shown in (**b**)) are red.

The structure of the dinuclear Ph_3PAuC_2pym complex is shown in Figure 4. The Au–Au distance of 3.0722(2) Å is well within the range typically considered for an aurophilic bonding interaction [31], leading to our interpretation of Ph_3PAuC_2pym as a dinuclear complex. All the atoms of the complex are crystallographically unique. Aurophilic interactions are common among Ph_3PAu complexes, though to our knowledge, there are only two examples in the CSD where aurophilic bonding occurs between Ph_3P–Au–C≡C fragments: bis[(thiphen-2-yl)ethynyl]-bis(triphenylphosphine)-di-gold (CSD refcode VULBIQ, Au–Au = 3.144 Å, [32]) and bis(μ2-penta-1,4-diyn-3-one)-tetrakis(triphenylphosphine)-tetra-gold (CSD refcode XIKWOF, Au–Au = 2.983 Å, [33]). The Ph_3PAuC_2pym complex has similar features about its Au centers to those other multinuclear complexes, namely approximately linear P–Au–C angles of 179.33(9)° and 173.11(9)°, Au–P distances of 2.2790(8) Å and 2.2788(7) Å, and Au–C distances of 1.998(3) Å and 1.996(3) Å.

The Ph_3PAuC_2pym complexes pack sufficiently well to not create large solvent-accessible voids (Figure 5a). In particular, one phenyl group of a Ph_3PAuC_2pym complex fits between the two pyrimidyl groups of a neighboring complex to form chains of the complexes propagating along the *b*-axis via C–H···N interactions (Figure 5b). Additional C–H···N and complementary C–H···π interactions assist the formation of these chains. Numerous other C–H···π interactions extend the packing structure to three dimensions.

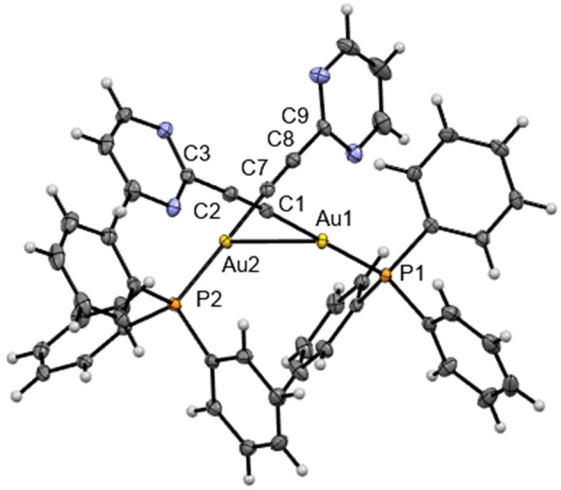

Figure 4. Crystal structure of Ph_3PAuC_2pym shown as displacement ellipsoids at 50% probability levels.

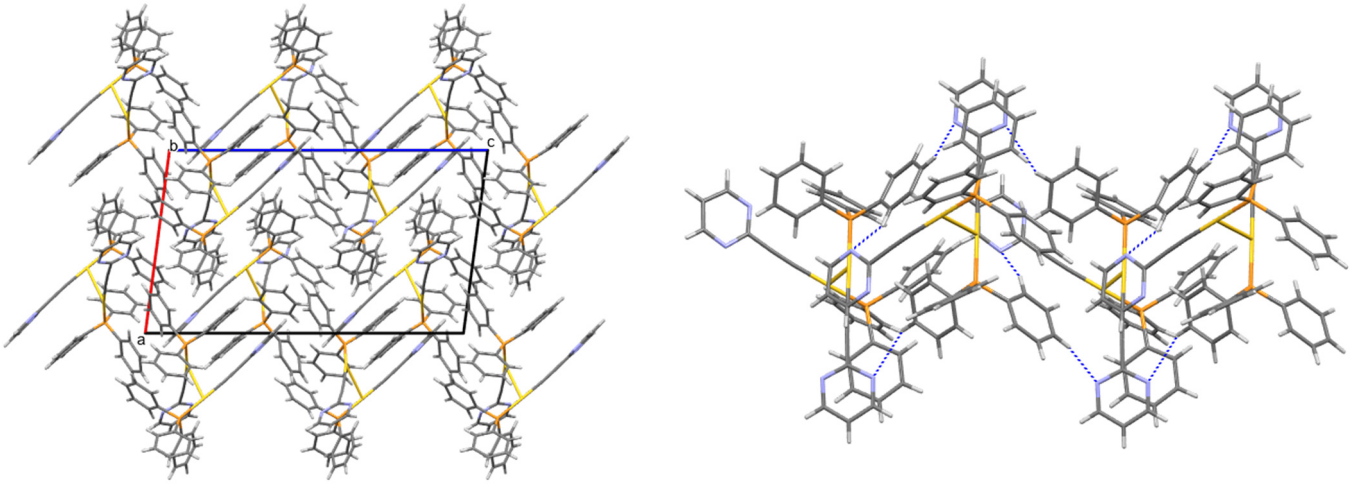

(**a**) (**b**)

Figure 5. Packing of dinuclear complexes in Ph_3PAuC_2pym: (**a**) Packing diagram viewed along *b*-axis. (**b**) Selected intermolecular interactions in Ph_3PAuC_2pym resulting in formation of chains propagating along *b*-axis via C–H···N (dashed blue lines). Carbon atoms are gray, nitrogen atoms are purple, gold atoms are yellow, and phosphorus atoms are orange.

The Cy_3PAuC_2pym complex crystallized as a mononuclear gold complex (Figure 6) with one unique complex in the asymmetric unit. It exhibits similar features of linear P–Au–alkyne connectivity (P–Au–C angle of 176.36(4)°, Au–P distance of 2.2936(4) Å, and Au–C distance of 2.0044(16) Å) to other Cy_3PAu complexes [21]. The use of 2-ethynylpyrimidine in the present study is again unique in the structural literature for Cy_3PAu complexes. Here, it again enables the formation of C–H···N interactions from one pyrimidyl group of a complex to one of the pyrimidyl nitrogen atoms of a neighboring complex, thereby creating chains along the *b*-axis (Figure 7a). The PCy_3 groups of neighboring chains are then positioned for localized complementary packing, which again limits the solvent-accessible void space (Figure 7b). Both of these features bear some similarity to what occurs in the (2-(4′-pyridyl)ethynyl)-(tris(cyclohexyl)phosphine)–gold complex (CSD refcode MUPGUZ, [21]), albeit with a generally shorter C···N distance across the C–H···N interactions of Cy_3PAuC_2pym (3.562(2) Å with C–H···N of 151.2° compared to 3.916(7) Å with C–H···N of 172.6°).

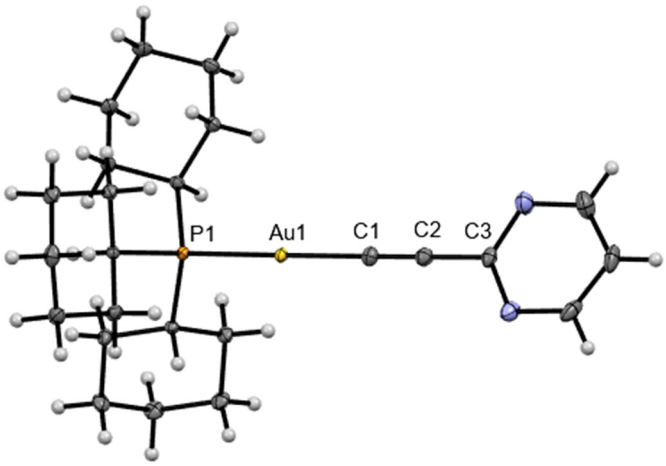

Figure 6. Crystal structure of Cy_3PAuC_2pym shown as displacement ellipsoids at 50% probability levels.

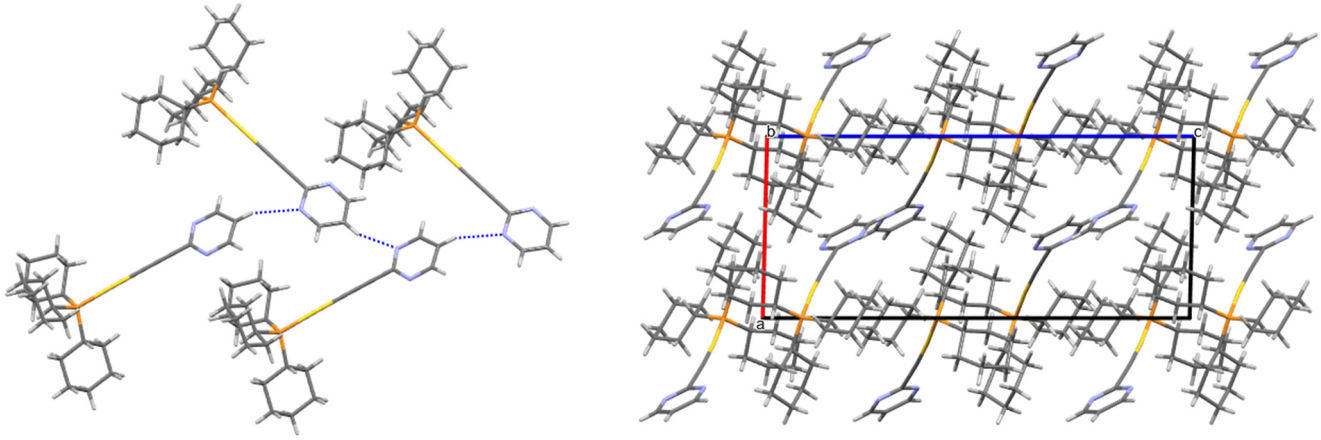

(**a**) (**b**)

Figure 7. Packing of complexes in Cy_3PAuC_2pym: (**a**) Selected intermolecular interactions in Cy_3PAuC_2pym resulting in formation of chains propagating along *b*-axis via C–H···N (dashed blue lines). (**b**) Packing diagram of Cy_3PAuC_2pym viewed along *b*-axis. Carbon atoms are gray, nitrogen atoms are purple, gold atoms are yellow, and phosphorus atoms are orange.

3.3. Characterization of the Alkynyl Pyrimidine Compounds

^{1}H-NMR spectroscopy served as an initial indicator that ^{t}bpyPt$(C_2pym)_2$, Ph_3PAuC_2pym, and Cy_3PAuC_2pym were successfully synthesized. A key feature in all the spectra was the presence of a downfield doublet and triplet integrating in a 2:1 ratio indicative of the resonances on the pyrimidine ring. Elemental analyses confirmed the purity of all three species, and crystallographic characterization (vide infra) supported the proposed structures with full structural characterization.

UV-Vis, excitation, and emission spectra of ^{t}bpyPt$(C_2pym)_2$, Ph_3PAuC_2pym, and Cy_3PAuC_2pym were collected in CH_2Cl_2. Over the range of concentrations where data were collected, no indication of ground-state aggregation was observed as indicated by Beer's law plots (Supplementary Materials). For each sample, the excitation spectra reasonably match the absorption spectra (Supplementary Materials), which indicates that the emission is not resultant of an impurity.

The UV-Vis spectra of ^{t}bpyPt$(C_2pym)_2$ contain transitions analogous to previously reported compounds of the form ^{t}bpyPt$(C_2R)_2$ (Supplementary Materials). The low-energy band (λ_{max} = 377 nm) was assigned as a charge-transfer transition based on previously reported Pt(II) alkynyl compounds [4]. Lu et al. reported that this band is blue-shifted in CH_2Cl_2

when electron withdrawing groups are appended on the acetylide substituents, as indicated by the comparison of ^{t}bpyPt($C_2$2-thio)$_2$ (where HC$_2$2-thio = 2-ethynylthiophene), which has a λ_{max} = 410, and the more electron-deficient ^{t}bpyPt($C_2C_6F_5$)$_2$, which has a λ_{max} = 381 nm [4]. The emission λ_{max} of ^{t}bpyPt(C_2pym)$_2$ at 512 nm (Figure 8) is blue-shifted relative to the previously reported ^{t}bpyPt($C_2$2-py)$_2$, namely due to the -C_2pym ligand being more electron-deficient than the -$C_2$2-py ligand. The emission spectra of ^{t}bpyPt(C_2pym) are unaffected by the presence of oxygen, unlike the R_3PAu(C_2pym) species (vide infra).

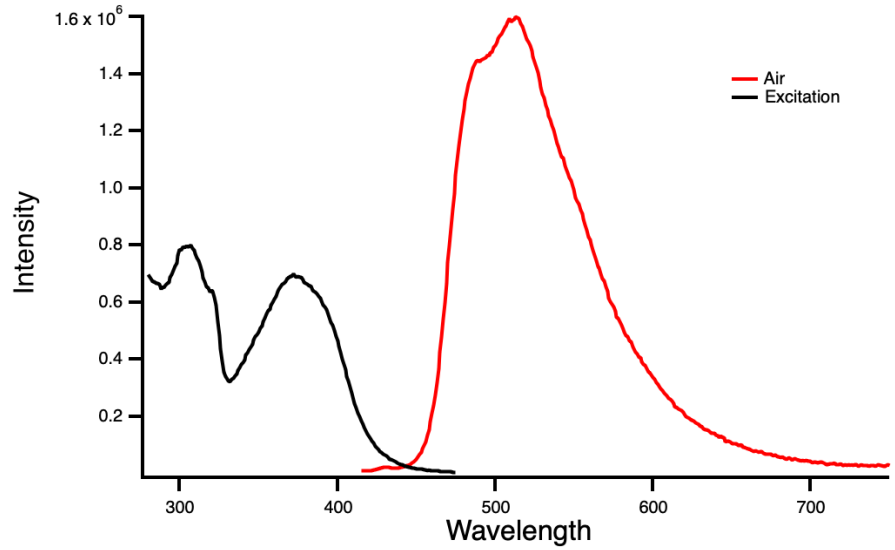

Figure 8. Excitation and emission spectra of ^{t}bpyPt(C_2pym)$_2$.

Regarding the Au(I) compounds, the UV-Vis spectra of both species (Supplementary Materials) show a low-energy feature (λ_{max} = 275 nm) assigned to an intraligand [$\pi \rightarrow \pi^*$ (C≡C)] transition based on the assignment for the previously synthesized Ph_3PAu($C_2$4-py) complex (where HC$_2$4-py = 4-ethynylpyridine) [34]. The higher-energy transitions were tentatively assigned to phosphine-centered intraligand (IL) transitions because these features are also observed in the precursor complexes, e.g., Ph_3PAuCl [35–38]. The emission spectra of Ph_3PAuC_2pym (Supplementary Materials) and Cy_3PAuC_2pym (Figure 9) are similarly structured with an emission λ_{max} = 434 nm for Ph_3PAuC_2pym and emission λ_{max} = 435 nm for Cy_3PAuC_2pym. In both Au(I) species, there is approximately a 10-fold increase in emission intensity upon purging with argon.

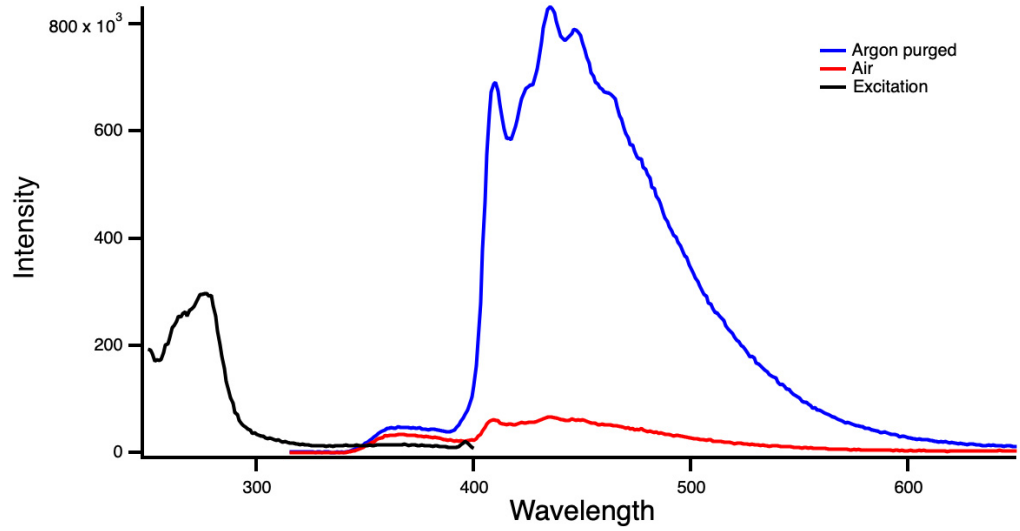

Figure 9. Excitation and emission spectra of Cy_3PAuC_2pym.

4. Conclusions

Three new transition metal complexes bearing 2-ethynylpyrimidine ligands have been synthesized, structurally characterized by X-ray crystallography, and further characterized by excitation and emission spectroscopy to gauge the utility of the alkynyl ligands toward tuning the emissive properties of complexes. The complexes, ^{t}bpyPt(C_2pym)$_2$, Ph_3PAuC_2pym, and Cy_3PAuC_2pym, were synthesized by the deprotonation of HC_2pym in the presence of ^{t}bpyPtCl_2, Ph_3PAuCl, and Cy_3PAuCl, respectively, to form the mixed-ligand species. The ^{t}bpyPt(C_2pym)$_2$ complex is a square planar Pt(II) complex with three unique complexes in the asymmetric unit that form stacks along the *b*-axis. The Ph_3PAuC_2pym complex forms a dinuclear Au(I) complex of two linear Ph_3PAuC_2pym units joined through aurophilic bonding. The Cy_3PAuC_2pym is likewise a linear Au(I) complex, but without aurophilic interactions, thus crystallizing as a discrete complex. Of note, the emission of the ^{t}bpyPt(C_2pym)$_2$ compound is blue-shifted relative to the previously reported ^{t}bpyPt($C_2$2-py)$_2$ complex, indicating that the introduction of electron-deficient heteroatoms provides a means of tuning of the optical properties of emissive alkynyl compounds. This provides an alternative strategy to the use of fluorinated alkynes, mainly -$C_2C_6F_5$, that are commonly utilized to blue-shift emission. Other pyrimidine derivatives (e.g., 2-ethynyl-5-fluoropyrimidine [39]) should be considered as ligands to blue-shift emission of transition metal compounds.

Supplementary Materials: The following supporting information can be downloaded at: https://www.mdpi.com/article/10.3390/cryst14070587/s1, Figure S1: ^{1}H-NMR of ^{t}bpyPt(C_2pym)$_2$ in $CDCl_3$, Figure S2: ^{1}H-NMR of Ph_3AuC_2pym in d_6-acetone, Figure S3: ^{1}H-NMR of Cy_3PAuC_2pym in $CDCl_3$, Figure S4: UV-Vis of ^{t}bpyPt(C_2pym)$_2$ and Beer's law plot, Figure S5: UV-Vis of Ph_3PAuC_2pym and Beer's law plot, Figure S6: UV-Vis of Cy_3AuC_2pym and Beer's law plot, Figure S7: Excitation and emission spectra of Ph_3PAuC_2pym.

Author Contributions: Conceptualization, S.L.M. and J.A.P.; methodology, S.L.M., J.A.P. and C.D.M.; validation, C.D.M., S.L.M. and L.E.D.; formal analysis, C.D.M., S.L.M., P.S.W., M.J.M., J.A.P. and L.E.D.; investigation, S.L.M., C.D.M., M.J.M., P.S.W. and L.E.D.; resources, J.A.P., C.D.M. and P.S.W.; data curation, S.L.M., M.J.M., P.S.W., C.D.M. and J.A.P.; writing—original draft preparation, J.A.P. and C.D.M.; writing—review and editing, J.A.P., C.D.M., M.J.M., P.S.W., L.E.D. and S.L.M.; visualization, M.J.M., C.D.M. and J.A.P.; supervision, J.A.P., P.S.W. and C.D.M.; project administration, J.A.P. All authors have read and agreed to the published version of the manuscript.

Funding: PSW acknowledges support from the National Science Foundation under Grant No. 2055326. Any opinions, findings and conclusions or recommendations expressed in this material are those of the authors and do not necessarily reflect those of the National Science Foundation.

Data Availability Statement: The raw data supporting the conclusions of this article will be made available by the authors on request. CCDC 2359466–2359468 contain the supplementary crystallographic data for this paper. These data can be obtained from the CCDC, 12 Union Road, Cambridge CB2 1EZ, UK; Fax: +44-1223-336033.

Conflicts of Interest: The authors declare no conflicts of interest.

References

1. Fu, J.-Z.; Zhang, X.; Wang, J.-Y.; Zhang, L.-Y.; Chen, Z.-N. Syntheses and photophysical properties of cyclometallated iridium (III) acetylide complexes. *Inorg. Chem. Commun.* **2012**, *22*, 123–125. [CrossRef]
2. Turlington, M.D.; Pienkos, J.A.; Carlton, E.S.; Wroblewski, K.N.; Myers, A.R.; Trindle, C.O.; Altun, Z.; Rack, J.J.; Wagenknecht, P.S. Complexes with Tunable Intramolecular Ferrocene to Ti^{IV} Electronic Transitions: Models for Solid State Fe^{II} to Ti^{IV} Charge Transfer. *Inorg. Chem.* **2016**, *55*, 2200–2211. [CrossRef] [PubMed]
3. Long, N.J.; Williams, C.K. Metal Alkynyl σ Complexes: Synthesis and Materials. *Angew. Chem. Int. Ed.* **2003**, *42*, 2586–2617. [CrossRef]
4. Lu, W.; Chan, M.C.W.; Zhu, N.; Che, C.-M.; He, Z.; Wong, K.-Y. Structural Basis for Vapoluminescent Organoplatinum Materials Derived from Noncovalent Interactions as Recognition Components. *Chem. Eur. J.* **2003**, *9*, 6155–6166. [CrossRef] [PubMed]

5. Lu, W.; Mi, B.-X.; Chan, M.C.W.; Hui, Z.; Che, C.-M.; Zhu, N.; Lee, S.-T. Light-Emitting Tridentate Cyclometalated Platinum(II) Complexes Containing σ-Alkynyl Auxiliaries: Tuning of Photo- and Electrophosphorescence. *JACS* **2004**, *126*, 4958–4971. [CrossRef]
6. Lu, W.; Zhu, N.; Che, C.-M. Polymorphic Forms of a Gold(I) Arylacetylide Complex with Contrasting Phosphorescent Characteristics. *JACS* **2003**, *125*, 16081–16088. [CrossRef]
7. Tang, M.-C.; Chan, A.K.-W.; Chan, M.-Y.; Yam, V.W.-W. Platinum and Gold Complexes for OLEDs. *Top. Curr. Chem.* **2016**, *374*, 46. [CrossRef] [PubMed]
8. Monkman, A. Why Do We Still Need a Stable Long Lifetime Deep Blue OLED Emitter? *ACS Appl. Mater. Inter.* **2022**, *14*, 20463–20467. [CrossRef]
9. Li, C.; Zhang, K.; Luo, Y.; Yang, Y.; Huang, Y.; Jia, M.; He, Y.; Lei, Y.; Tang, J.-X.; Huang, Y.; et al. Realizing highly efficient deep-blue organic light-emitting diodes towards Rec.2020 chromaticity by restricting the vibration of the molecular framework. *Chem. Sci.* **2024**, *15*, 4790–4796. [CrossRef]
10. Siddiqui, I.; Kumar, S.; Tsai, Y.-F.; Gautam, P.; Shahnawaz; Kesavan, K.; Lin, J.-T.; Khai, L.; Chou, K.-H.; Choudhury, A.; et al. Status and Challenges of Blue OLEDs: A Review. *Nanomaterials* **2023**, *13*, 2521. [CrossRef]
11. He, R.; Xu, Z.; Valandro, S.; Arman, H.D.; Xue, J.; Schanze, K.S. High-Purity and Saturated Deep-Blue Luminescence from trans-NHC Platinum(II) Butadiyne Complexes: Properties and Organic Light Emitting Diode Application. *ACS Appl. Mater. Inter.* **2021**, *13*, 5327–5337. [CrossRef] [PubMed]
12. McCarthy, J.S.; McCormick, M.J.; Zimmerman, J.H.; Hambrick, H.R.; Thomas, W.M.; McMillen, C.D.; Wagenknecht, P.S. Role of the Trifluoropropynyl Ligand in Blue-Shifting Charge-Transfer States in Emissive Pt Diimine Complexes and an Investigation into the PMMA-Imposed Rigidoluminescence and Rigidochromism. *Inorg. Chem.* **2022**, *61*, 11366–11376. [CrossRef] [PubMed]
13. Li, K.; Ming Tong, G.S.; Wan, Q.; Cheng, G.; Tong, W.-Y.; Ang, W.-H.; Kwong, W.-L.; Che, C.-M. Highly phosphorescent platinum(II) emitters: Photophysics, materials and biological applications. *Chem. Sci.* **2016**, *7*, 1653–1673. [CrossRef] [PubMed]
14. Chow, P.-K.; To, W.-P.; Low, K.-H.; Che, C.-M. Luminescent Palladium(II) Complexes with π-Extended Cyclometalated [R–C^N^N–R] and Pentafluorophenylacetylide Ligands: Spectroscopic, Photophysical, and Photochemical Properties. *Chem. Asian J.* **2014**, *9*, 534–545. [CrossRef]
15. Tong, G.S.M.; Law, Y.-C.; Kui, S.C.F.; Zhu, N.; Leung, K.H.; Phillips, D.L.; Che, C.-M. Ligand-to-Ligand Charge-Transfer Transitions of Platinum(II) Complexes with Arylacetylide Ligands with Different Chain Lengths: Spectroscopic Characterization, Effect of Molecular Conformations, and Density Functional Theory Calculations. *Chem. Eur. J.* **2010**, *16*, 6540–6554. [CrossRef] [PubMed]
16. Rossi, E.; Colombo, A.; Dragonetti, C.; Righetto, S.; Roberto, D.; Ugo, R.; Valore, A.; Williams, J.A.G.; Lobello, M.G.; De Angelis, F.; et al. Tuning the Dipolar Second-Order Nonlinear Optical Properties of Cyclometalated Platinum(II) Complexes with Tridentate N^C^N Binding Ligands. *Chem. Eur. J.* **2013**, *19*, 9875–9883. [CrossRef] [PubMed]
17. Hudson, Z.M.; Sun, C.; Harris, K.J.; Lucier, B.E.G.; Schurko, R.W.; Wang, S. Probing the Structural Origins of Vapochromism of a Triarylboron-Functionalized Platinum(II) Acetylide by Optical and Multinuclear Solid-State NMR Spectroscopy. *Inorg. Chem.* **2011**, *50*, 3447–3457. [CrossRef] [PubMed]
18. Bordwell, F.G. Equilibrium acidities in dimethyl sulfoxide solution. *Acc. Chem. Res.* **1988**, *21*, 456–463. [CrossRef]
19. Keyworth, D. Notes: Basicity and Ionization Constants of Some Pyrazine Derivatives. *J. Org. Chem.* **1959**, *24*, 1355–1356. [CrossRef]
20. Albert, A.; Phillips, J.N. 264. Ionization constants of heterocyclic substances. Part II. Hydroxy-derivatives of nitrogenous six-membered ring-compounds. *J. Chem. Soc.* **1956**, 1294–1304. [CrossRef]
21. Chao, H.-Y.; Lu, W.; Li, Y.; Chan, M.C.W.; Che, C.-M.; Cheung, K.-K.; Zhu, N. Organic Triplet Emissions of Arylacetylide Moieties Harnessed through Coordination to $[Au(PCy_3)]^+$. Effect of Molecular Structure upon Photoluminescent Properties. *JACS* **2002**, *124*, 14696–14706. [CrossRef]
22. Zhong, F.; Zhao, J. An N^N Platinum(II) Bis(acetylide) Complex with Naphthalimide and Pyrene Ligands: Synthesis, Photophysical Properties, and Application in Triplet–Triplet Annihilation Upconversion. *Eur. J. Inorg. Chem.* **2017**, *2017*, 5196–5204. [CrossRef]
23. Su, H.; Wang, Y.; Ren, L.; Yuan, P.; Teo, B.K.; Lin, S.; Zheng, L.; Zheng, N. Fractal Patterns in Nucleation and Growth of Icosahedral Core of $[Au_nAg_{44-n}(SC_6H_3F_2)_{30}]^{4-}$ (n = 0–12) via ab Initio Synthesis: Continuously Tunable Composition Control. *Inorg. Chem.* **2019**, *58*, 259–264. [CrossRef]
24. Chan, K.T.; Tong, G.S.M.; To, W.-P.; Yang, C.; Du, L.; Phillips, D.L.; Che, C.-M. The interplay between fluorescence and phosphorescence with luminescent gold(I) and gold(III) complexes bearing heterocyclic arylacetylide ligands. *Chem. Sci.* **2017**, *8*, 2352–2364. [CrossRef]
25. *Apex3*; Bruker AXS Inc.: Madison, WI, USA, 2015.
26. Sheldrick, G.M. SHELXT—Integrated space-group and crystal-structure determination. *Acta Crystallogr. Sect. A Found. Adv.* **2015**, *71*, 3–8. [CrossRef]
27. Sheldrick, G.M. Crystal structure refinement with SHELXL. Acta Crystallogr. *Sect. C Struct. Chem.* **2015**, *71*, 3–8. [CrossRef] [PubMed]
28. Fernández, S.; Forniés, J.; Gil, B.; Gómez, J.; Lalinde, E. Synthesis, structural characterisation and photophysics of anionic cyclometalated bis(alkynyl)(benzo[h]quinolinate)platinate(II) species. *Dalton Trans.* **2003**, 822–830. [CrossRef]

29. Jaques, L.D.; McDarmont, S.L.; Smart, M.M.; McMillen, C.D.; Neglia, S.E.; Lee, J.P.; Pienkos, J.A. Structural characterization of the metalloligand tbpyPt($C_2$2-py)$_2$ and its interaction with Pd(OAc)$_2$. *Inorg. Chem. Commun.* **2020**, *112*, 107722. [CrossRef]
30. Shavaleev, N.M.; Bell, Z.R.; Easun, T.L.; Rutkaite, R.; Swanson, L.; Ward, M.D. Complexes of substituted derivatives of 2-(2-pyridyl)benzimidazole with Re(I), Ru(II) and Pt(II): Structures, redox and luminescence properties. *Dalton Trans.* **2004**, 3678–3688. [CrossRef]
31. Schmidbaur, H.; Schier, A. A briefing on aurophilicity. *Chem. Soc. Rev.* **2008**, *37*, 1931–1951. [CrossRef]
32. Zeman, C.J.I.V.; Shen, Y.-H.; Heller, J.K.; Abboud, K.A.; Schanze, K.S.; Veige, A.S. Excited-State Turn-On of Aurophilicity and Tunability of Relativistic Effects in a Series of Digold Triazolates Synthesized via iClick. *JACS* **2020**, *142*, 8331–8341. [CrossRef] [PubMed]
33. Armitt, D.J.; Bruce, M.I.; Morris, J.C.; Nicholson, B.K.; Parker, C.R.; Skelton, B.W.; Zaitseva, N.N. Bis(metallaethynyl) Ketones: Synthesis and Structure of {(Ph_3P)AuC≡C}$_2$CO and Attempted Transmetalation: Formation and Structure of [1,3-{Ru(dppe)Cp}$_2${c-COC(OMe)CHCCH}]PF_6. *Organometallics* **2011**, *30*, 5452–5456. [CrossRef]
34. Cheung, K.-L.; Yip, S.-K.; Yam, V.W.-W. Synthesis, characterization, electrochemistry and luminescence studies of heterometallic gold(I)–rhenium(I) alkynyl complexes. *J. Organomet. Chem.* **2004**, *689*, 4451–4462. [CrossRef]
35. Blanco, M.C.; Cámara, J.; Gimeno, M.C.; Jones, P.G.; Laguna, A.; López-de-Luzuriaga, J.M.; Olmos, M.E.; Villacampa, M.D. Luminescent Homo- and Heteropolynuclear Gold Complexes Stabilized by a Unique Acetylide Fragment. *Organometallics* **2012**, *31*, 2597–2605. [CrossRef]
36. Li, D.; Hong, X.; Che, C.-M.; Lo, W.-C.; Peng, S.-M. Luminescent gold(I) acetylide complexes. Photophysical and photoredox properties and crystal structure of [{Au(C≡CPh)}$_2$(μ-$Ph_2PCH_2CH_2PPh_2$)]. *J. Chem. Soc. Dalton Trans.* **1993**, 2929–2932.
37. Yam, V.W.-W.; Choi, S.W.-K.; Cheung, K.-K. Synthesis and Design of Novel Tetranuclear and Dinuclear Gold(I) Phosphine Acetylide Complexes. First X-ray Crystal Structures of a Tetranuclear ([Au_4(tppb)(C∶CPh)$_4$]) and a Related Dinuclear ([Au_2(dppb)(C∶CPh)$_2$]) Complex. *Organometallics* **1996**, *15*, 1734–1739. [CrossRef]
38. Yam, V.W.-W.; Cheung, K.-L.; Yuan, L.-H.; Wong, K.M.-C.; Cheung, K.-K. Synthesis, structural characterization and binding studies of a novel dinuclear gold(I) calix[4]crown acetylide complex. *Chem. Commun.* **2000**, 1513–1514. [CrossRef]
39. Xu, L.; Hartz, R.A.; Beno, B.R.; Ghosh, K.; Shukla, J.K.; Kumar, A.; Patel, D.; Kalidindi, N.; Lemos, N.; Gautam, S.S.; et al. Synthesis, Structure–Activity Relationships, and In Vivo Evaluation of Novel Tetrahydropyran-Based Thiodisaccharide Mimics as Galectin-3 Inhibitors. *J. Med. Chem.* **2021**, *64*, 6634–6655. [CrossRef]

Disclaimer/Publisher's Note: The statements, opinions and data contained in all publications are solely those of the individual author(s) and contributor(s) and not of MDPI and/or the editor(s). MDPI and/or the editor(s) disclaim responsibility for any injury to people or property resulting from any ideas, methods, instructions or products referred to in the content.